Numerical techniques for the inversion of Eddy Current Testing data

Guglielmo Rubinacci and Antonello Tamburrino
Dipartimento di Ingegneria Industriale - Università degli studi di Cassino, Cassino, Italy

Abstract – **In this paper, we discuss two techniques for the reconstruction of conductivity profiles in the low frequency limit. The first one is based on the second order approximation of the scattered field operator. In the second procedure, the problem is linearized at the expense of an increase in the number of unknowns including, in this case, the current density and the electric field. Some simple 2D examples are presented to point out and compare the main features of the two approaches.**

I. Introduction

Eddy Current Testing (ECT) is a well known method for the electromagnetic inspection of conducting materials. From the computational point of view, one has to deal with a direct and an inverse problem. The direct problem consists in the evaluation of the scattered field at the measurement probe locations, for a given exciting field and conductivity profile. In the inverse problem, one has to find the conductivity profile, with the measurements and the excitations being known quantities. The inverse problem is non-linear and ill-posed. Usually, the model is linearized in the neighborhood of a known conductivity background σ_0; therefore, the electric field inside the conducting domain is approximated by the values obtained for $\sigma=\sigma_0$, assuming that the unknown part of the profile $\Delta\sigma$, often limited to a small flawed region, introduces only a small negligible perturbation. This is the so-called first order Born approximation that gives rise to the class of linear methods. In this paper, we briefly discuss the limits of this linear approximation, showing that it fails to identify profiles varying fast spatially.

A better approximation can be obtained using a higher order expansion of the scattered field. In particular, the adoption of a second order approximation already allows to substantially enlarge the class of conductivity profiles that can be identified. A further improvement can be achieved sometimes by noticing that the approximation error depends upon the difference between the unknown conductivity and a reference profile assumed as the initial point of the expansion. Hence, the error in the expansion can be iteratively reduced by choosing, as initial point, the solution obtained in the previous step of the procedure.

The quadratic approach has been already used in [1]-[2]. In particular, in [1] the main aspects of the method have been introduced with reference to a model based on the 2D integral equation for the electric field. In [2], the approach has been extended to an integral 3D formulation in terms of the electric vector potential **T**. In that case, the functional expansion was in terms of the electric resistivity. Moreover, the advantage of iterating the expansion during the optimization procedure was demonstrated with reference to simple test cases.

Here, we compare this quadratic approach to a different method that takes advantage of the particular structure of the mathematical model under investigation. In particular, the model contains the product of the conductivity and the electric field inside the specimen. As a consequence, the problem can be linearized at the expense of a further increase in the number of field variables, by considering as unknowns both the current density and the electric field. In this case, after estimating the fields inside the specimen, the conductivity is computed as the solution of the constitutive equation in a proper functional space.

Some simple 2D examples will be discussed to point out and compare the main features of these two approaches.

II. The Direct Problem

Consider a non magnetic conducting domain V_c characterized by the conductivity profile $\sigma(\mathbf{r})$. Assuming a sinusoidal excitation, the mathematical model of the problem is described in the frequency domain by the following classic integral formulation:

$$\mathbf{E}(\mathbf{r}) = \mathbf{E}^{inc}(\mathbf{r}) + (A_i \underline{\sigma}\mathbf{E})(\mathbf{r}), \quad \forall \mathbf{r} \in V_c \tag{1}$$

$$\mathbf{E}^s(\mathbf{r}_m) = (A_e \underline{\sigma}\mathbf{E})(\mathbf{r}_m), \qquad \forall \mathbf{r}_m \in S_m. \tag{2}$$

Here **E** is the electric field, $\mathbf{E}^{inc}$ is the applied electric field due to a suitable system of excitation, S_m is the discrete set of points where the measurements are taken, A_i is the classic integral operator giving the electric field inside V_c associated to the current density $\mathbf{J}=\sigma\mathbf{E}$ flowing in V_c. The integral operator A_e, analogously defined, gives the electric field in S_m due to the current density flowing in V_c; finally $\underline{\sigma}$ is an operator that, applied to **E**, gives $\sigma\mathbf{E}$ and it is defined as:

$$\underline{\sigma}: \mathbf{E} \in \mathbf{L}^2(V_c) \to \sigma\mathbf{E} \in \mathbf{L}^2(V_c). \tag{3}$$

Restricting the attention, for the sake of simplicity, to the two dimensional scalar case, the electric field is assumed to be directed along the z axis and the integral operators assume the following form:

$$A_i : J \in L^2(V_c) \to -j\omega\mu_0 \int_{V_c} G(k|\mathbf{r}-\mathbf{r}'|) J(\mathbf{r}')\mathrm{dv}, \quad \forall \mathbf{r} \in V_c \tag{4}$$

Manuscript received September 23, 1996.
G. Rubinacci, e-mail rubinacci@ing.unicas.it, fax 0039 776 310812;
A. Tamburrino, e-mail tambur@ing.unicas.it.
This work was supported in part by MURST and CNR of Italy.

$$A_e : J \in L^2(V_c) \to -j\omega\mu_0 \int_{V_c} G(k|\mathbf{r}-\mathbf{r}'|) J(\mathbf{r}')\mathrm{dv}, \quad \forall \mathbf{r} \in S_m \tag{5}$$

Here k is the wave number, G is the scalar Green's function in the free space and $\omega \in \Omega$, the set of frequencies imposed by the system of excitation.

III. The Inverse Problem and The Quadratic Approach

In the inverse problem, the conductivity profile is unknown and it should be reconstructed on the basis of the knowledge of the electric or magnetic field at a set of measurement points for given frequencies and excitations. The inverse problem is non-linear and ill-posed. It can be conveniently formulated as the minimization with respect to $\sigma(\mathbf{r})$ of the error functional:

$$\Phi[\sigma] = \sum_{k=1}^{M} \left\| E_k^s[\sigma] - \tilde{\mathbf{E}}_k \right\|^2 \tag{6}$$

where $\{\tilde{\mathbf{E}}_1, \ldots, \tilde{\mathbf{E}}_M\}$ is the set of M noisy measurements of the scattered field at the measurement points $(\mathbf{r}_1, \omega_1), \ldots, (\mathbf{r}_M, \omega_M)$, respectively, $E^s[\sigma]$ is a nonlinear operator mapping the conductivity profile into the scattered field for a given system of excitation and $E_k^s[\sigma]$ is the value of $E^s[\sigma]$ at the point $(\mathbf{r}_k, \omega_K)$. The operator $E^s[\sigma]$ is defined as:

$$E^s[\sigma] = A_e \underline{\sigma} (I - A_i \underline{\sigma})^{-1} E^{inc}.$$

The solution can be obtained by expanding $E^s[\sigma]$ in the neighborhood of a known background conductivity $\sigma_0(\mathbf{r})$. This approach was initially proposed for the phase retrieval and the reconstruction of dielectric permittivity profiles in [3]-[5] and extended to the study of Eddy Current Testing problems in [1]-[2]. Here, we briefly recall the basic aspects of the method. Setting σ as $\sigma=\sigma_0+\Delta\sigma$, where $\Delta\sigma$ is a "small perturbation", $E^s[\sigma]$ can be approximated as:

$$E_{1,k}^s[\sigma] = E_k^s[\sigma_0] + A_k[\Delta\sigma] \tag{7}$$

$$E_{2,k}^s[\sigma] = E_k^s[\sigma_0] + A_k[\Delta\sigma] + B_k[\Delta\sigma, \Delta\sigma] \tag{8}$$

where $A_k[\Delta\sigma]$ is a linear operator and $B_k[\Delta\sigma_1, \Delta\sigma_2]$ is a bilinear operator, defined as:

$$A_k[\Delta\sigma] = A_e\left[\underline{\sigma}_0 (I - A_i \underline{\sigma}_0)^{-1} A_i + I\right] \underline{\Delta\sigma}\, E_0 \tag{9}$$

$$B_k[\Delta\sigma_1, \Delta\sigma_2] = A_e\left[\underline{\sigma}_0 (I - A_i \underline{\sigma}_0)^{-1} A_i + I\right] \underline{\Delta\sigma}_1 \cdot (I - A_i \underline{\sigma}_0)^{-1} A_i \underline{\Delta\sigma}_2\, E_0 \tag{10}$$

with E_0 being the electric field associated to the background conductivity σ_0:

$$E_0 = (I - A_i \underline{\sigma}_0)^{-1} E^{inc} \tag{11}$$

Notice that the linear approximation is consistent with the zero order approximation of the electric field in S_c. Instead, the quadratic expansion requires the first order term in the approximated expression of the electric field in S_c. This allows to take into account the reaction field inside S_c associated to the variations $\Delta\sigma$ of the unknown conductivity profile. This contribution is relevant when the skin depth is of the same order of the characteristic dimensions of the domain and it allows to enlarge the interval of frequencies where the approximation holds. Thus, an increased number of independent equations are available with respect to the linear case at the expense of a slight increase of the complexity of the system that becomes nonlinear. Notice also that the fast space varying components of the profile are filtered out by the integral operators in the linear case, whereas their effect is detectable in the higher order approximations.

A discrete approximation of these operators can be obtained by assuming $\Delta\sigma \in \Sigma = \mathrm{span}\,\{f_1, \ldots, f_N\}$ where $f_1, \ldots, f_N$ is a set of linearly independent base functions for $\Delta\sigma$ such as:

$$\Delta\sigma(\mathbf{r}) = \sum_k c_k f_k(\mathbf{r}) \tag{12}$$

Then

$$E_{2,k}^s[\sigma_0 + \mathbf{f}^T\mathbf{c}] = E_k^s[\sigma_0] + [A_k]\mathbf{c} + \mathbf{c}^T\{B_k\}\mathbf{c} \tag{13}$$

where $[A_k]_i = A_k[f_i]$, $\{B\}_{i,j} = B_k[f_i, f_j]$, $\mathbf{c}^T = [c_1, \ldots, c_N]$ and $\mathbf{f}^T = [f_1, \ldots, f_N]$.

IV. The Quasi-Linear Approach

The bilinear form of the mathematical model can be further exploited. To this purpose we rewrite the system in the following form:

$$A_e \mathbf{J} = \mathbf{E}^s \tag{14}$$

$$\mathbf{E} = \mathbf{E}^{inc} + A_i \sigma \mathbf{E} \tag{15}$$

$$\mathbf{J} = \sigma \mathbf{E} \tag{16}$$

where $\mathbf{E}^s$ is the scattered field. Then, we discretize eqs (14)-(15)-(16), by choosing suitable weighting and shape functions, thus obtaining

$$\{A_e\}[J] = [E^s] \tag{17}$$

$$[E] = [E^{inc}] + \{A_i\}[J] \tag{18}$$

$$[J] = \{\underline{\sigma}\}[E]. \tag{19}$$

$\{Ae\}$, $\{Ai\}$ and $\{\underline{\sigma}\}$ are the matrices representing the integral operators A_e, A_i and the operator $\underline{\sigma}$, respectively, while $[J]$ and $[E]$ are the vectors made of the components of $\mathbf{J}$ and $\mathbf{E}$ associated to the chosen shape functions. To simplify the notation, a single excitation is considered in the following, since the extension to multiple excitations is straightforward.

The first two equations form an ill-conditioned linear system in $[J]$ and $[E]$. In fact, only a number of components of $[J]$, related to the pattern of singular values of $\{A_e\}$, can be reconstructed in a reliable way. The solution of (19) provides the unknown conductivity profile. This model has been studied in [6]-[7] for the reconstruction of permittivity profiles. There, the knowledge associated to the background is not taken into account and all the equations are discretized using pulse shape functions and a point matching approach. In [7], a solution of (17) is first obtained by means of the pseudo-inversion of the operator A_e. Then, (18) gives an estimate of $[E]$ and finally σ is obtained solving (19) by a point matching approach. Here we analyze this method showing how it can be conveniently improved. To this purpose, the system (17)-(19) is rewritten as

$$\{A_e\}\left(I-\{\underline{\sigma}_0\}\{A_i\}\right)^{-1}[J^*]=[\Delta E]^s \triangleq [E^s]-[E_0^s] \tag{20}$$

$$[E]=[E_0]+\left(I-\{A_i\}\{\underline{\sigma}_0\}\right)^{-1}\{A_i\}[J^*] \tag{21}$$

$$[J^*]-\{\underline{\Delta\sigma}\}[E]=[0] \tag{22}$$

where $[E_0]=\left(I-\{A_i\}\{\underline{\sigma}_0\}\right)^{-1}[E^{inc}]$ and $[E_0^S]=\{A_e\}\{\underline{\sigma}_0\}[E_0]$. Note that to compute $[\Delta E]$ the pseudo-inversion of the matrix $\{A_e\}\left(I-\{\underline{\sigma}_0\}\{A_i\}\right)^{-1}$ is required which has a slightly better conditioning than the matrix $\{A_e\}$.

To solve (22), once $[J^*]$ and $[E]$ are estimated by means of (20) and (21), respectively, we expand Δσ as in (12), so that $\{\underline{\Delta\sigma}\}=\sum_k c_k\{f_k\}$.

The key point is to project the constitutive equation on a suitable basis. In fact, the reconstructed field variables show strong fluctuations due to the difficulty of reconstructing the fast space varying components. The information related to these components is meaningless and should be filtered out. A natural basis is associated to the singular value decomposition $\{U,\Lambda,V\}$ of the matrix $\{A_e\}\left(I-\{\underline{\sigma}_0\}\{A_i\}\right)^{-1}$, i.e. $\{A_e\}\left(I-\{\underline{\sigma}_0\}\{A_i\}\right)^{-1}=\{U\}\{\Lambda\}\{V\}^+$.

By projecting (22) on the right singular vectors and using (20) we have

$$[u_i]^+[\Delta E^s]-\sum_k \lambda_i\{V\}^+\{f_k\}[E]c_k=0, \forall i=1,\ldots,N_r \tag{23}$$

with N_r being the number of singular values above a suitable threshold. The linear system (23) is over-determined since $N_r\cdot N_{inc}/2>N$ and is solved by means of a pseudo inversion.

With this approach we have obtained a significant improvement of the quality of reconstruction in comparison to the previous one as it will be shown in the numerical experiment presented in the next section.

V. The Model Problem

We refer to a indefinite hollow cylinder, whose cross section is a thin circular crown, excited by a system of currents directed along its axis. The eigenvalues of the operators A_e and A_i can be computed analytically [8]. Their expressions are:

$$a_n^e=-j\frac{\omega\mu R_c}{2}\frac{1}{|n|}\left(\frac{R_c}{R_m}\right)^{|n|}, \quad \forall n\neq 0$$

$$a_0^e=-j2\omega\mu_0R_c\pi\left(-\frac{\pi}{2}\ln(kR_m)-\frac{j}{4}\right)$$

$$a_n^i=-j\frac{\omega\mu R_c}{2}\frac{1}{|n|}, \quad \forall n\neq 0$$

$$a_0^i=-j2\omega\mu_0R_c\pi\left(-\frac{\pi}{2}\ln(kR_c)-\frac{j}{4}\right)$$

Notice that the eigenvalues of A_e go to zero as n goes to infinity so that the scattered field, in presence of noise, can be described with a finite number of parameters. Assuming that the available set of excitations is finite, the information to reconstruct the profile is limited to a finite number of equations. Hence only a finite number of unknown coefficients can be reconstructed in a reliable way.

We assume for Σ the space spanned by the first N_θ Fourier harmonics. In this case, it is very useful to expand also the fields in terms of sinusoidal shape functions, the eigenfunctions of the operators A_e and A_i. It follows that the system of equations can be rewritten in the following form:
of the background σ_0, since its euclideian norm $||\Delta\sigma||$ is much smaller than $||\sigma_0||$. The discretized model is made of 21×7×2 real equations obtained with N_e=7 excitations at the frequency f=10kHz and N_m=21 complex field measurements. The profile is approximated by the first N_θ=10 Fourier harmonics (21 real unknowns).

$$a_n^eJ_n=E_n^s$$

$$E_n=E_n^{inc}+a_n^i\sum_k\sigma_{n-k}E_k$$

$$J_n=\sum_k\sigma_{n-k}E_k\ ,$$

VI. Numerical Results

The main parameters of the numerical experiment are defined in Fig. 1 and their numerical values are reported in Table I. In particular, the incident field is produced by two filamentary conductors, carrying equal and opposite sinusoidal currents and located at $R=R_e$, $\theta=\theta_e\pm\Delta\theta_e/2$; the couple of source currents is sequentially placed around the cylinder axis, taking N_e series of measurements ($\theta_e=(i-1)2\pi/N_e$, $i=1, \ldots, N_e$). The field measurements are taken at $R_i=R_m$, $\theta_i=(i-1)2\pi/N_m$, $i=1, \ldots, N_m$. A typical profile is described by a rectangular pulse of width Δθ and amplitude $\Delta\sigma_M$ on a constant background σ_0 as shown in Fig. 2.

The first example aims to show the improvement on the Born approximation given by the quadratic term. In Fig. 3, we show the results of the reconstruction using a linear and a quadratic approach, respectively. The profile has a width Δθ=30°, an amplitude $\Delta\sigma_M$=−1 MS/m, on a background

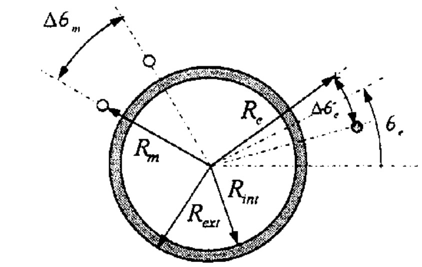

Probe ○
Source Currents ⊗ +

Fig. 1. Geometry of the model problem.

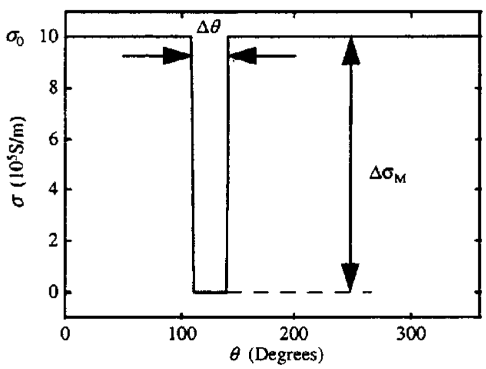

Fig. 2. The reference conductivity profile.

σ_0=1MS/m. Notice that $\Delta\sigma$ is a relatively small perturbation of the background σ_0, since its euclideian norm $||\Delta\sigma||$ is much smaller than $||\sigma_0||$. The discretized model is made of 21×7×2 real equations obtained with N_e=7 excitations at the frequency f=10kHz and N_m=21 complex field measurements. The profile is approximated by the first N_θ=10 Fourier harmonics (21 real unknowns). The physical constraint $\sigma \geq 0$ has not been taken into account in order to take advantage of the simple mathematical structure of the error functional. In Fig. 4, the results obtained for the same reference case but solved with the "quasi-linear" approach are shown. In this case the unknown current density and electric field are discretized using 101 Fourier harmonics.

In Fig. 5, we show the current density and the electric field as reconstructed by solving eqs. (20)-(21) and compared with the true (numerically computed) values.

In Fig. 6, the conductivity profile provided by eq. (23) and by a point matching solution of eq. (16) using a single excitation are reported. The anomalous spike in Fig. 6b is due to the errors in the estimation of the current density in correspondence of the electric field zero crossing.

To understand the different features of the two approaches, we remark that, in case of the functional expansion, the series

Table I

MAIN PARAMETERS OF MODEL PROBLEM

Parameter	Value	Parameter	Value
R_{ext}	0.025 m	R_e/R_{ext}	1.02
R_{in}	0.024 m	N_m	21
$\Delta\theta_e$	60°	N_e	7
R_m/R_{ext}	1.02	f	10kHz

is convergent if the Euclidean norm of the matrix $\{S\} = \left(I - \{A_i\}\{\underline{\sigma}_0\}\right)^{-1}\{A_i\}\{\underline{\Delta\sigma}\}$ is less than unity. In the "quasi-linear" method, the conditioning of the matrix $\{A_{ql}\} = \{A_e\}\left(I - \{\underline{\sigma}_0\}\{A_i\}\right)^{-1}$ is responsible for the quality of the reconstruction. In both cases, the high frequency components of the profiles are the most difficult to be identified because of the spatial filtering introduced by the integral operators. To support these theoretical considerations

a)

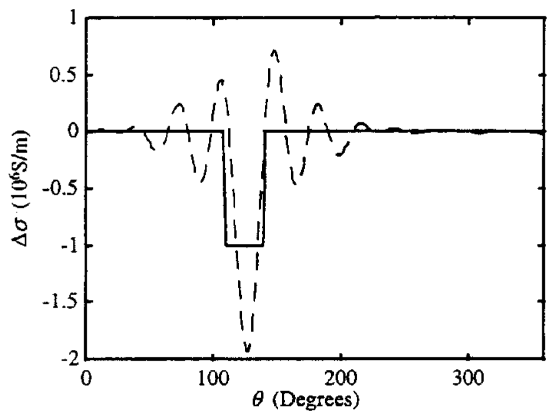

b)

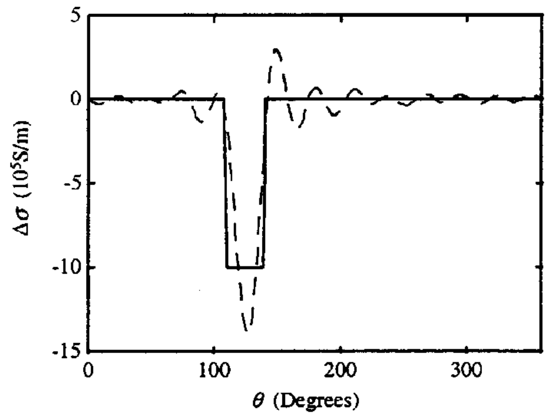

Fig. 3. The conductivity $\Delta\sigma$ (dashed line) obtained using the linear (a) and the quadratic (b) approach, compared with the unknown profile (solid line).

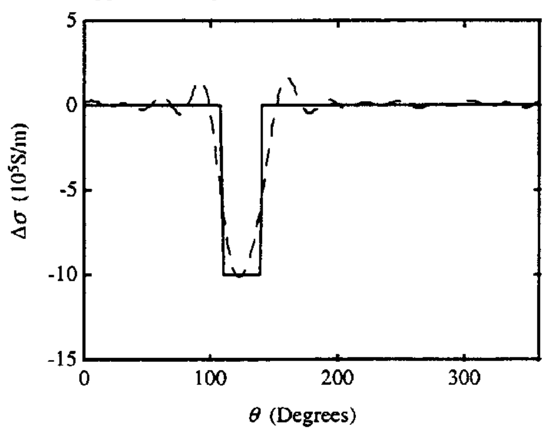

Fig. 4. The conductivity $\Delta\sigma$ (dashed line) obtained using the "quasi-linear" approach, compared with the unknown profile (solid line).

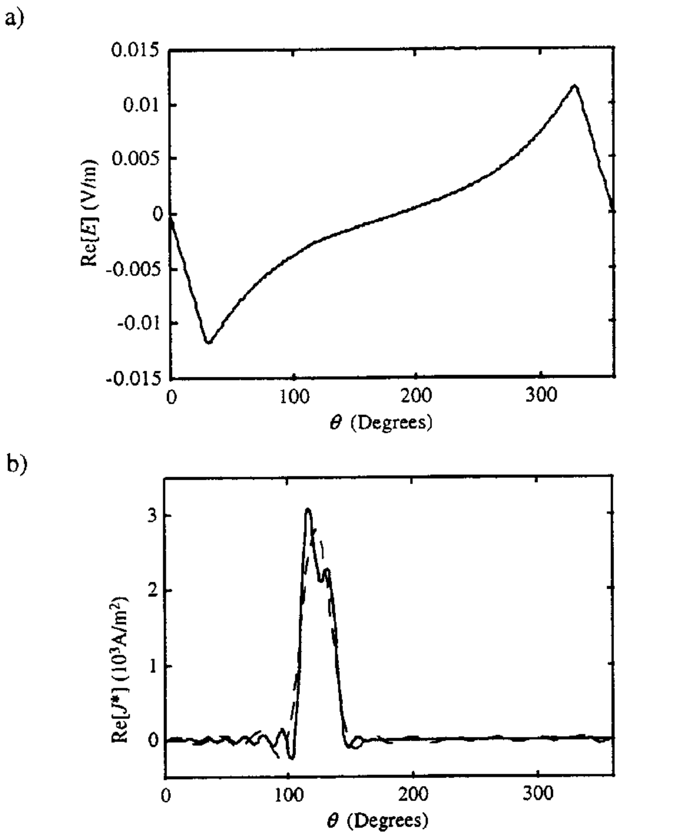

Fig. 5. The real part (solid line) of the electric field (a) and the current density J^* (b), respectively, and their reconstruction obtained using the "quasi-linear" approach (dashed line).

we performed several numerical experiments varying once at the time three parameters, the frequency f affecting the conditioning of $\{A_{ql}\}$, and $\Delta\theta$ and $\Delta\sigma_M$ influencing the norm of the matrix $\{S\}$. In Fig. 7, we show the profiles as identified by means of the "quasi-linear" procedure, assuming a frequency of f=100Hz, lower than in the reconstruction shown in Figs 3-4. Because the conditioning of $\{A_{ql}\}$ improves with f, better results are obtained with the "quasi-linear" method at higher frequencies. To further clarify this point, in Fig. 8, we show the normalized singular values of $\{A_e\}$ and $\{A_{ql}\}$ for the two frequencies. It can be seen that, at f=100Hz, the two patterns are practically coincident whereas at f=10kHz $\{A_{ql}\}$ has a better conditioning than $\{A_e\}$. The quadratic approach has a dual behavior, since the error increases with the frequency as a result of the increasing of the norm of $\{S\}$. In Figs. 9 and 10, we show the results obtained for $\Delta\sigma_M$=10MS/m and $\Delta\theta$=60°, respectively. The reconstruction via the quadratic approach becomes more difficult since the norm of $\{S\}$ increases with $\Delta\theta$ and $\Delta\sigma_M$.

VII. Conclusions

The objective of this paper was to discuss the main characteristics of two different approaches for the reconstruction of conductivity profiles. The first one is based on the second order approximation of the scattered field operator. In the second procedure, the problem is linearized at the expense of an increase in the number of unknowns, including, in this case, the current density and the electric field.

It has been shown that the introduction of the quadratic term in the expansion of the scattered field improves the quality of the reconstruction especially in case of fast spatially varying profiles. The main limitation of the method is related to the convergence of the expansion and hence to

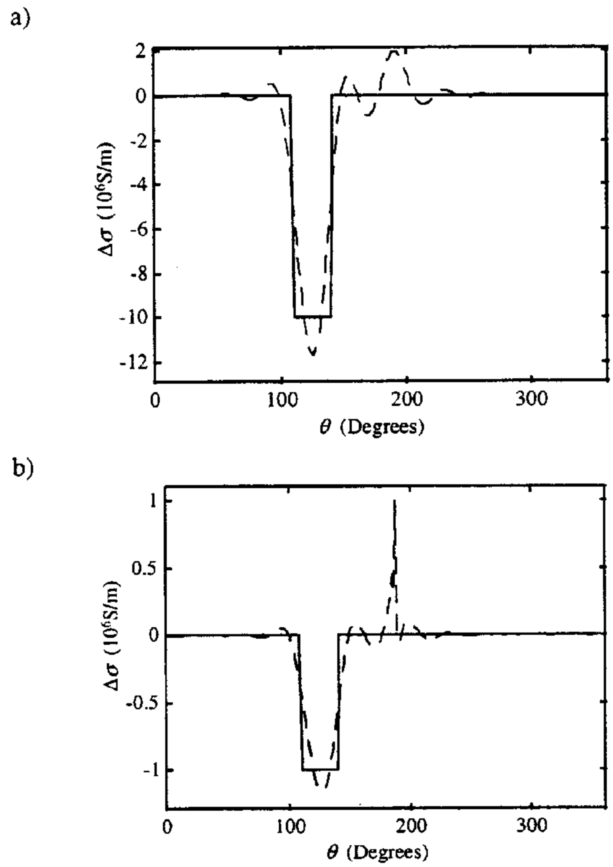

Fig. 6. The conductivity Δσ (dashed line) obtained using the "quasi-linear" approach with a single excitation, compared with the unknown profile (solid line). a) Singular functions projection. b) Point matching.

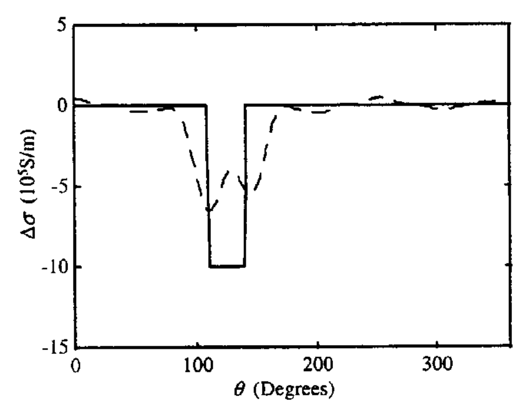

Fig. 7. The conductivity Δσ (dashed line) obtained using the "quasi-linear" approach with f=100Hz, compared with the unknown profile (solid line).

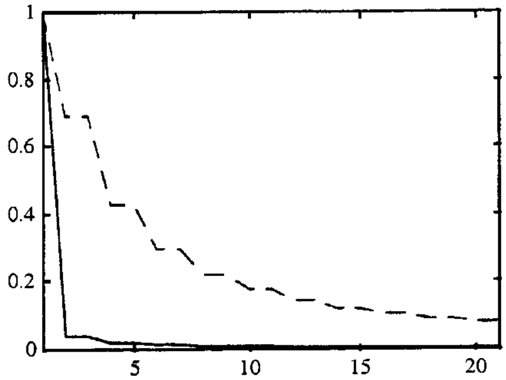

Fig. 8. The singular values pattern for the matrices $\{A_e\}$, $\{A_{ql}\}$ at f=100Hz and for the matrix $\{A_e\}$ at f=10kHz (solid line) compared to the pattern for the matrix $\{A_{ql}\}$ at f=10kHz (dashed line).

a)

b)

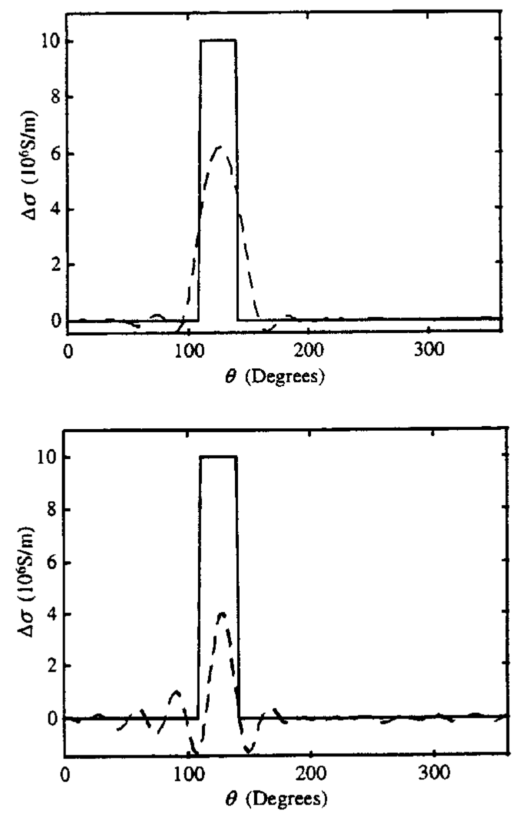

Fig. 9. The conductivity $\Delta\sigma$ (dashed line) obtained using the "quasi-linear" (a) and the quadratic (b) approach with $\Delta\sigma$=10MS/m, compared with the unknown profile (solid line).

the norm of the matrix $\{S\}$. Larger norms introduce higher errors in the approximation of the field. Another critical issue is related to the presence of local minima. The particular structure of the second order operator can be conveniently used to avoid (at least in principle) their presence [3]-[5].

The "quasi-linear" approach, on the other hand is limited by the conditioning of the matrix $\{A_{ql}\}$, affecting any reconstruction procedure. It has been shown that the conditioning can be conveniently improved by introducing the knowledge of the conductivity background.

Although further investigations are required for testing the

a)

b)

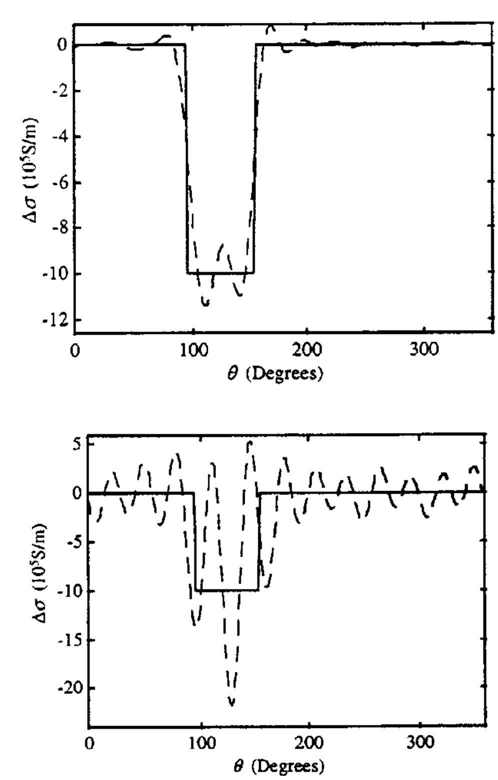

Fig. 10. The conductivity $\Delta\sigma$ (dashed line) obtained using the "quasi-linear" (a) and the quadratic (b) approach with $\Delta\theta$=60°, compared with the unknown profile (solid line).

procedures in more realistic and complex three-dimensional geometries, the knowledge gained by this theoretical analysis and a number of 2D tests allows us to conclude that both techniques can be efficiently used for the reconstruction of conductivity profiles.

REFERENCES

[1] R. Pierri, G. Rubinacci, A. Tamburrino, "A quadratic approach for the reconstruction of conductivity profiles using eddy currents", *IEEE Trans. Magn.*, Vol. 32, No. 3, 1996, pp. 1310-1313.

[2] R. Pierri, G. Rubinacci, A. Tamburrino, 'A numerical algorithm for the reconstruction of 3D conductivity profiles using eddy currents testing', Studies in Applied Electromagnetics and Mechanics, R. Collins et al. editors, IOS Press, 1995.

[3] T. Isernia, G. Leone, R. Pierri, "Phaseless near field techniques: formulation of the problem and field properties," *Journal of Electromagnetic Waves and Application*, Vol. 8, No. 7, 871-888, 1994.

[4] T. Isernia, G. Leone, R. Pierri, "Phaseless near field techniques: uniqueness conditions and attainment of the solution," *Journal of Electromagnetic Waves and Application*, Vol. 8, No. 7, 889-908, 1994.

[5] A. Brancaccio, V. Pascazio, R. Pierri: "A Quadratic Model for Inverse Profiling: the One-Dimensional Case", *Journal of Electromagnetic waves and applications*, Vol. 9, No. 4, 1995, pp 673-696.

[6] M.M. Ney, A.M. Smith, S.S. Stuchly: "A Solution of Electromagnetic Imaging Using Pseudoinverse Transformation", *IEEE Trans. Medical Imaging*, Vol. 3, No. 4, December 1984, pp 155-162.

[7] S. Caorsi, E. Capra, G.L. Gragnani, A. Massa, M. Pastorino: "Microwave imaging in the Spatial Domain for Canonical Dielectric Objects", *IEEE Trans. Magn.*, Vol. 31, No. 3, 1995, pp. 1562-1565.

[8] A. Tamburrino: "Sulla ricostruzione di profili di conducibilità con metodi non lineari", PhD Thesis, in italian, Politecnico di Torino, February 1996.